NRIAG Journal of Astronomy and Geophysics 7 (2018) 309–317

Contents lists available at ScienceDirect

NRIAG Journal of Astronomy and Geophysics

journal homepage: www.elsevier.com/locate/nrjag

Full length article

3D Electrical Resistivity Imaging (ERI) for subsurface evaluation in pre-engineering construction site investigation

Olawale Olakunle Osinowo*, Michael Oluseyi Falufosi

Department of Geology, University of Ibadan, Ibadan, Oyo-State, Nigeria

ARTICLE INFO

Keywords:
Engineering structure
Foundation rocks
Spatial variability
Georesistivity imaging
Quartz-schist

ABSTRACT

Three Dimensional (3D) Electrical Resistivity Imaging (ERI) was carried out for pre-construction foundation investigation of a proposed engineering construction site within the University of Ibadan Campus, south-western Nigeria, where some distressed structures (offices and hostels) have been reported to show stress induced cracks attributed to incompetent foundation support from rocks upon which they were constructed.

The 3D grid of resistivity data generated along parallel and equally spaced profiles stations presented the resistivity distribution of the subsurface as well as delineated zones of relatively high resistivity values (450–4500 Ω m) in the east and lower resistivity zones (15–300 Ω m) in the west. The study also delineates zones of isolated low resistivity values (10–50 Ω m) at the mid and west end of the field. The generated resistivity distribution sections, maps and 3D model indicate spatial variation in resistivity value which varies both laterally and vertically. The variation which is attributed to differences imposed by underlying rock's structural and geological rock composition resulted from complex rock coexistence as schist (quartz- and amphibolitic-schist) and quartzite coexist as underlying rocks of the proposed construction site, especially since these rocks respond to weathering differently.

The generated subsurface resistivity model guided selection of geotechnical investigation points which captures spatial variation in subsurface physical properties as recorded by the measured subsurface resistivity. Better guided geotechnical investigation provided needed information required to design appropriate foundation support for the proposed engineering structure.

1. Introduction

The success of engineering structures which are directly established on the surface of the earth is among other factors dependent on the support offered by the foundation materials that bear the load of the structure (Terzaghi et al., 1996). The ability of foundation rocks to offer necessary bearing support for engineering structures depend on the bearing capacity of the rock(s). Geological and structural factors such as mineralogical composition, rock fabric, rock association, degree of weathering, fluid saturation, rock deformation and occurrence of joints and faults would not only define the bearing strength of the foundation rocks, it could also impact spatial variability in the strength of the foundation material arising from heterogeneity in rock's physical properties (Fishman, 1979). Spatial variability in rock bearing capacity is known to impact stress on the poorly supported engineering structures with associated failure which could occur as total, partial and differential settlement or even total collapse of the structure (Nobahar & Popescu, 2001; El-Kateb et al., 2003; Cho, 2007).

The prevalent occurrence of failed and collapse buildings and other distressed engineering structures in Nigeria with associated loss of lives and properties has necessitated the need to ensure that engineering structures are properly constructed (Ede, 2010). While much attention has been focused on proper engineering design, structural balance, reinforcement, material quality among others, less effort has been channelled to ascertain the integrity of the foundation material that would support the structure. Hence common occurrence of many stress induced cracks and other foundation related defect features on different public and private engineering structures, some of which are simply disasters waiting to occur (Folagbade, 2001; Osinowo et al., 2011; Matawal, 2012).

Geophysical investigation offers a cheaper and faster means of getting detailed and credible information about the subsurface. Different geophysical techniques possess ability to image the ground in terms of rock association, distribution and structural deformation,

Peer review under responsibility of National Research Institute of Astronomy and Geophysics.
* Corresponding author.
E-mail address: wale.osinowo@ui.edu.ng (O.O. Osinowo).

https://doi.org/10.1016/j.nrjag.2018.07.001
Received 18 November 2017; Received in revised form 20 May 2018; Accepted 4 July 2018
Available online 09 July 2018

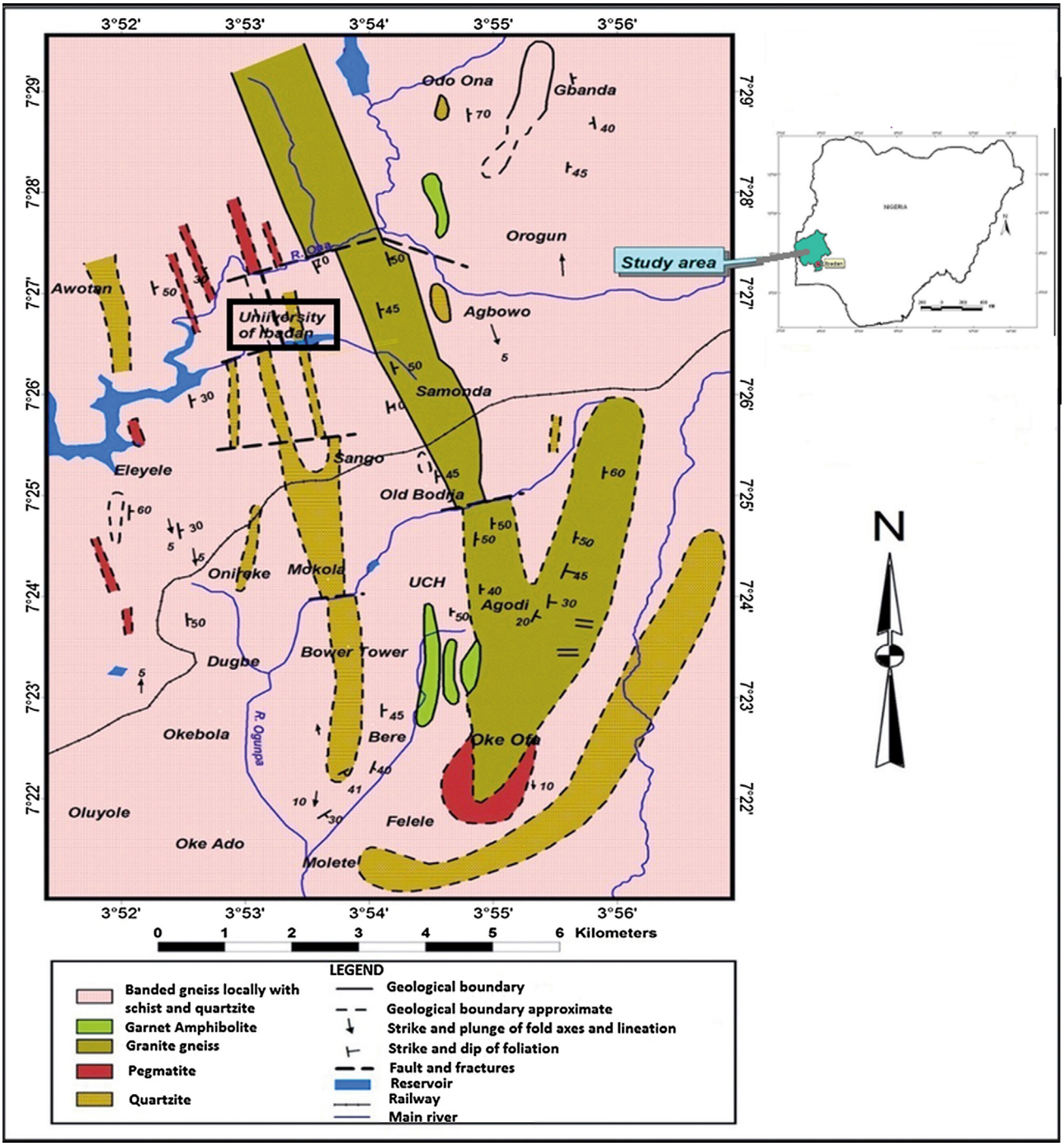

Fig. 1. The geological map of Ibadan and environs (modified after Amanambu, 2015).

which offer credible information regarding the support in term of strength that a foundation rock is likely to offer to engineering structures (Olorunfemi & Mesida, 1987; Palacky, 1987; Olayanju et al., 2017). Electrical Resistivity Imaging (ERI) technique has been very effective in illuminating the subsurface and apt at providing information about the rock physical properties for economical, environmental and engineering purposes (Keller & Frischknecht, 1966). Different electrical data acquisition technique as well as electrode and profile configurations have been described to present different desirable subsurface imaging abilities (Telford et al., 1990; Sharma, 1997). Three dimensional (3D) ERI geophysical investigation approach offers ability to characterise the subsurface as well as determine heterogeneity in measured rock properties along the vertical (z) and the two orthogonal horizontal (x & y) directions. The determination of variation in foundation rock's properties along the three orthogonal directions affords the ability to evaluate the spatial variation in rock strength as imposed by the heterogeneity of rock properties as they vary from place to place (Badmus et al., 2012).

In this study, 3D ERI technique was applied as a pre-engineering construction investigation tool to study a proposed construction site within the University of Ibadan campus, Ibadan, southwestern Nigeria. The study evaluated the suitability of the site's foundation rocks to offer necessary foundation support to the proposed engineering structure, which become particularly essential due to the prevalence of some distressed engineering structures (office complexes and students hostels), commonly characterised with numerous stress induced cracks,

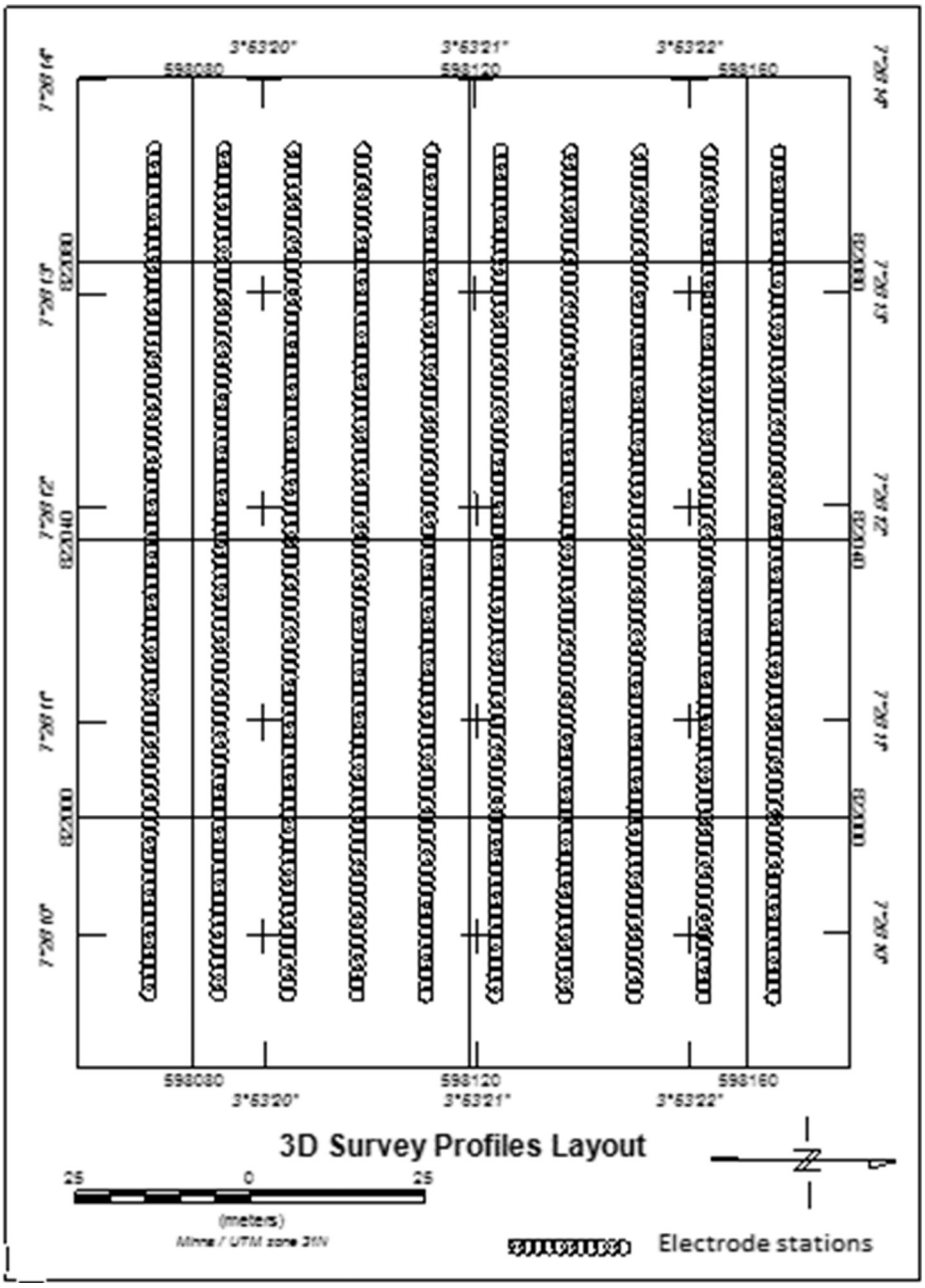

Fig. 2. 3D resistivity survey profile layout showing parallel equal-spaced profiles.

within the campus. The occurrence of stress induced cracks on these distressed buildings have been shown through investigations to be related to the incompetent foundation rocks which fail to offer required support for the entire or part of building due to variation in rock strength imposed by heterogeneity. The complex rock association of Quartz-schist, Amphibolitic-schist and Quartzite rocks underlain by Biotite and Granite Gneiss often predisposes buildings constructed, especially in the southern parts of the University of Ibadan campus to foundation support challenges as these different rock units present different support capacity to the structure founded on them.

This study infer the spatial variability in rock's strength generated by heterogeneity in rock's physical properties due to both lateral and vertical variations in rock physical properties measured through subsurface georesistivity investigation along carefully established parallel equally spaced resistivity profiles lines. Through this study, useful information as regards distribution of rock's physical properties shown by the variation of the measured electrical resistivity are generated and used to guide the design of the structures' foundation.

2. Location and the Geology of the Study Area

The study area is a proposed building construction site within the University of Ibadan Campus, in Ibadan, southwestern Nigeria. The site is located in the southwestern part of the University campus, and situated between latitude 7° 26.00[1]N and 7° 27.7[1]N and longitudes 3° 53.00[1]E and 3° 54.12[1]E in the north western part of Ibadan. The geology of Ibadan and environs has been well described (Jones & Hockey, 1964: Grant, 1971; Burke et al, 1976) to consist mainly of metasediment series with associated metaigneous rocks, classified to belong to the Migmatite - Gneiss Complex (MGC) of the Basement Complex of southwestern Nigeria (Burke & Dewey, 1972).

The Basement Complex of southwestern Nigeria consists predominantly of metasedimentary, minor metaigneous, metavolcanic rocks and older granite series which comprises of Schists, Quartzites,

Banded and Granite Gneisses and interbedded amphiboles generated from metamorphism of shales, grewackes and sandstones with interbedded basalts (Oyawoye, 1972; Rahaman, 1976). Evidence of Pan African Orogeny and later tectonic imprints have been reported and they are impressed on rocks as folds, faults, rock foliation and schistocity around Ibadan and environs (Burke et al, 1976; Shakleton, 1976).

Field mapping was carried out around the University of Ibadan campus to identify different rocks types and complex rock associations as well as some structural elements around the study area. The dominant rock types include quartz-schist, amphibolitic-schist, quartzite, granite and banded gneisses which dominantly trend along approximately north–south direction. Minor rocks also identified include dolerite and amphibolites. The granite and banded gneisses are generally observed to be mostly low lying and underlay the schist rocks and quartzite which often occur as ridges. The quartzite rocks present clear evidence of schistocity. Other visible tectonic imprints include joints, faults, folds and foliation of gneisses rocks, evident as alternation of dark and light minerals (Burke & Dewey, 1972). The geology of Ibadan and environ showing the University of Ibadan campus as the study area is presented in Fig. 1.

3. Materials and methods

A carefully designed data acquisition procedure was adopted in this study to generate grid of information which were systematically measured to present the variation of ground electrical resistivity along three orthogonal directions. Ground apparent resistivity measurement was carried out using multi-electrode Supersting R8/IP/SP Geo-electrical resistivity meter which has ability to make simultaneous measurements with the aid of built-in internal transmitter and AGI electrode Switch box. This automatically switches between electrodes aligned along the established profile for rapid measurement. Resistivity measurements were carried out along ten (10) established equally spaced resistivity profiles which were 10 m apart. Eighty four (84) geo-referenced electrode stations were occupied on each profile line at 3 m station interval using dipole-dipole electrode configuration (Fig. 2). Dipole-dipole electrode configuration is able to overcome resistivity measurement challenges arising from electrode polarization as a result of reasonable separation between the current and potential electrodes (Sasaki, 1989; White et al., 2003). The electrode configuration is also capable of high integrity data measurement at depth and thus able to generate high resolution electrical resistivity data. Fig. 2 presents the 3D profile layout and the pictures while occupying different profile lines during surveys are presented in Fig. 3.

Ground resistivity measurement involves injecting current (I) into the ground across two current electrodes which are firmly driven into the ground. One of the electrodes act as a sink (−I) for current injection into the ground while the second acts as a return (+I) into the current injecting source and thus guarantee current flow within the subsurface. The resultant potential difference (V) generated due to the flow of injected current is measured via two potential electrodes which are separated by a distance that corresponds to a factor (n) of the spacing (a) between individual current or potential electrodes. A measure of ground resistance to current flow is computed as the ratio of the generated ground voltage resulting from flow of current within the subsurface. The computed ground resistance is converted to apparent ground resistivity (ρa) by incorporating the geometric factor as $(n(n+1)(n+2)\pi a)$ of the electrode measurement configuration (Eq. (1)) (Telford et al., 1990; Sharma, 1997)

$$\rho a = n(n+1)(n+2)\frac{V}{I}\pi a \quad (1)$$

The integrity of the generated apparent ground resistivity data from the geophysical survey was ascertained and the data also evaluated for consistency. Subsequently the data were filtered to clean out spurious and spiky data having no geologic relevance. The cleaned data were thereafter inverted using RES2DINV inversion algorithm developed by Loke & Baker, (1996) to generate 2D resistivity distribution model of the subsurface which consist of noise free (reduced to barest minimum) and depth matched resistivity data (Loke, 2000 & 2001; Loke et al., 2013). This is achieved through the forward modeling subroutine of RES2DINV which calculates the theoretical apparent ground resistivity values based on a non-linear least squares optimisation (Sasaki, 1989; DeGroot-Hedlin & Constable, 1990; Auken & Christiansen, 2004). A high quality result with characteristic low RMS value (< 5%) usually obtained after four (4) to six (6) iterations indicate low degree of misfit between the observed and the theoretical model and thus reflect the integrity of the generated model as a representation of the subsurface across the sampled profiles.

The resulting inverted data from the generated 2D geo-resistivity models were sorted based on corresponding profiles into depth locations using 45° depth point projection from the surface current and potential electrodes' mid points. The sorted data were geo-referenced with the aid of the individual electrode's Global Positioning System (GPS) readings of the established electrode points. All the geo-referenced inverted resistivity data from all the ten (10) profiles were combined and gridded using 3D kriging gridding algorithm extension of Geosoft to generate 3D inverse resistivity model of the subsurface (Olea, 1974; Swain, 1976; Webring, 1981). This presents variation in ground resistivity along and across the established profiles stations as well as show variation in ground resistivity with depth. The generate 3D inverse resistivity model was further smoothened to generate the distribution of ground resistivity across the proposed engineering construction site.

4. Results and Interpretations

The subsurface resistivity investigation of proposed engineering construction site generated 2D resistivity models, sections, resistivity distribution depth maps as well as 3D resistivity model of the subsurface. The 2D resistivity distribution models which were generated by inverting the resistivity data acquired from individual profiles present variation in ground resistivity along the occupied electrode stations within each profile. The models present variations in ground resistivity value from near the surface to a depth of about 30 m.

All the 2D resistivity models (Fig. 4) apart from profile 1 presented three layers, which appear relatively well developed (layers well defined) at the centre and the western end of the W–E running profiles with the near surface (0–1.5 m) constituting the first layer. The near surface resistivity distribution indicate highly heterogeneous unit with resistivity value ranging from low (< 10 Ω m) through medium (20–450 Ω m) to high resistivity value (> 1500 Ω m). The middle layer presents characteristically low resistivity values (8–157 Ω m), which appear very prominent at the centre and western end of the studied field. The thickness of the low resistivity zone varies from less than 3 m to about 17 m.

The third (lower) layer presents relatively high resistivity value (> 450 Ω m), higher than that of the second (middle) layer. The resistivity of the third layer increases with depth except in profile 6 where low resistivity unit is encountered at depth of about 28 m. Relatively high resistivity value (> 1650 Ω m) characterises the eastern end (right end) of all the profiles which indicate relatively high resistive section of the field.

The 2D resistivity sections generated from combined inverted resistivity data obtained from the study area also reflect variation in ground resistivity with depth. Georesistivity sections generated along E–W and N–S directions, parallel and perpendicular to the occupied profile stations respectively are presented in Fig. 5 (a & b). The sections generally indicate higher ground resistivity in the eastern end of the field, while the western end presents relatively lower resistivity distribution. The low resistivity zones as shown by the E–W and N–S (Fig. 5 (a & b) appear to divide the field into two, where the low

Fig. 3. Profiles layout for ERI survey.

resistivity distribution zone appears restricted to the west. The prominent low resistivity zone observed on the N–S trending georesisitivity sections (Fig. 5b) which occurs at the centre of the field is more extensive along the north south directions but generally decreases westward.

A resistivity distribution mesh which combines both the N–S and E–W trending sections (Fig. 6) also confirmed higher resistivity distribution pattern in the east (> 650 Ω m) relative to the west

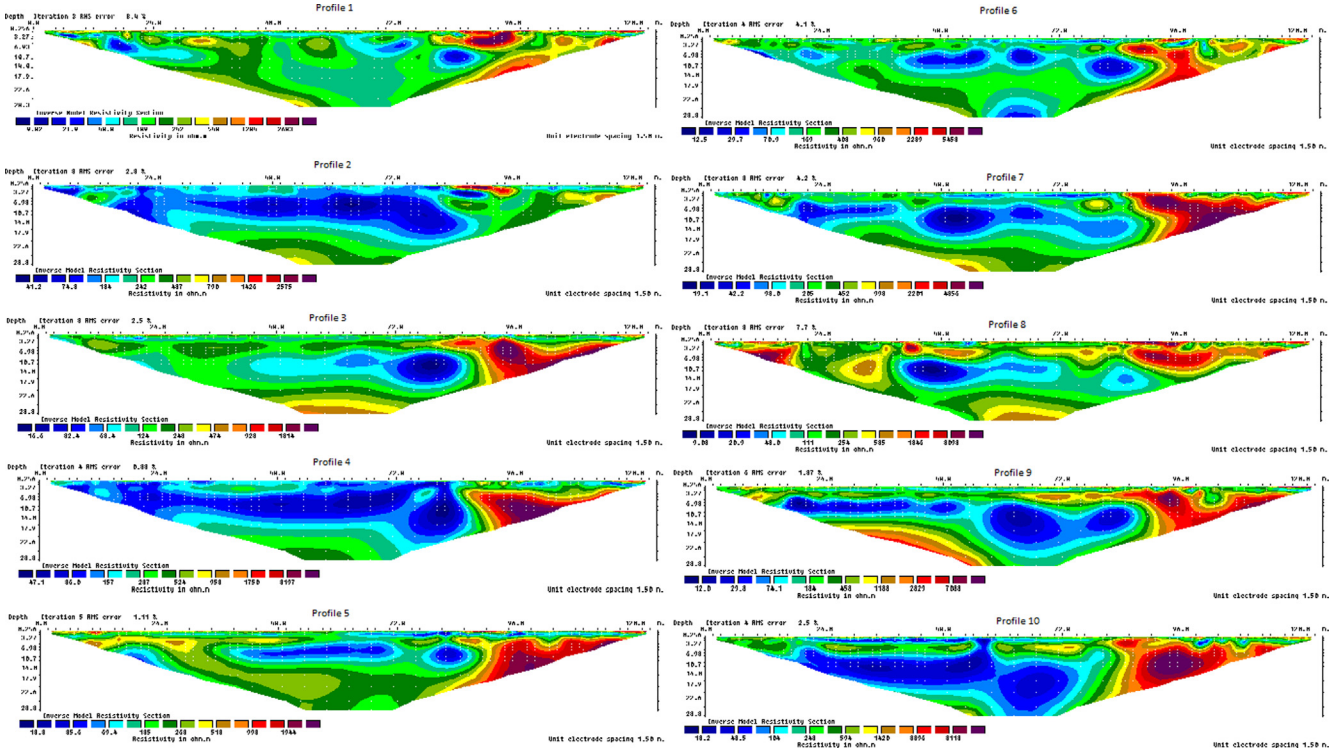

Fig. 4. 2D inverted resistivity models of occupied profiles at the study area.

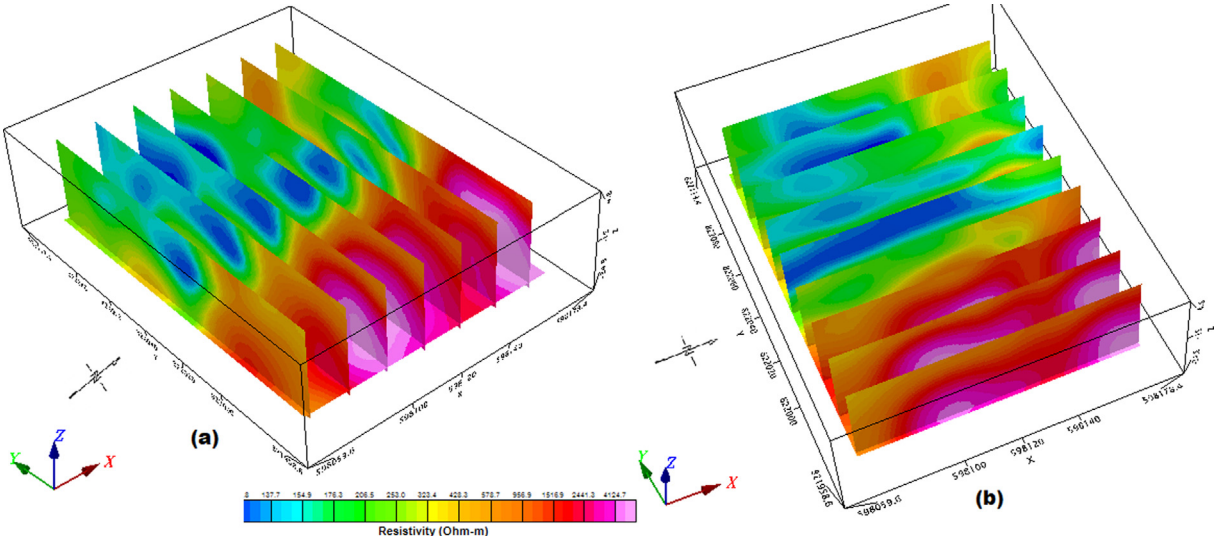

Fig. 5. (a) E–W and (b) N–S trending 2D georesistivity sections across the study area.

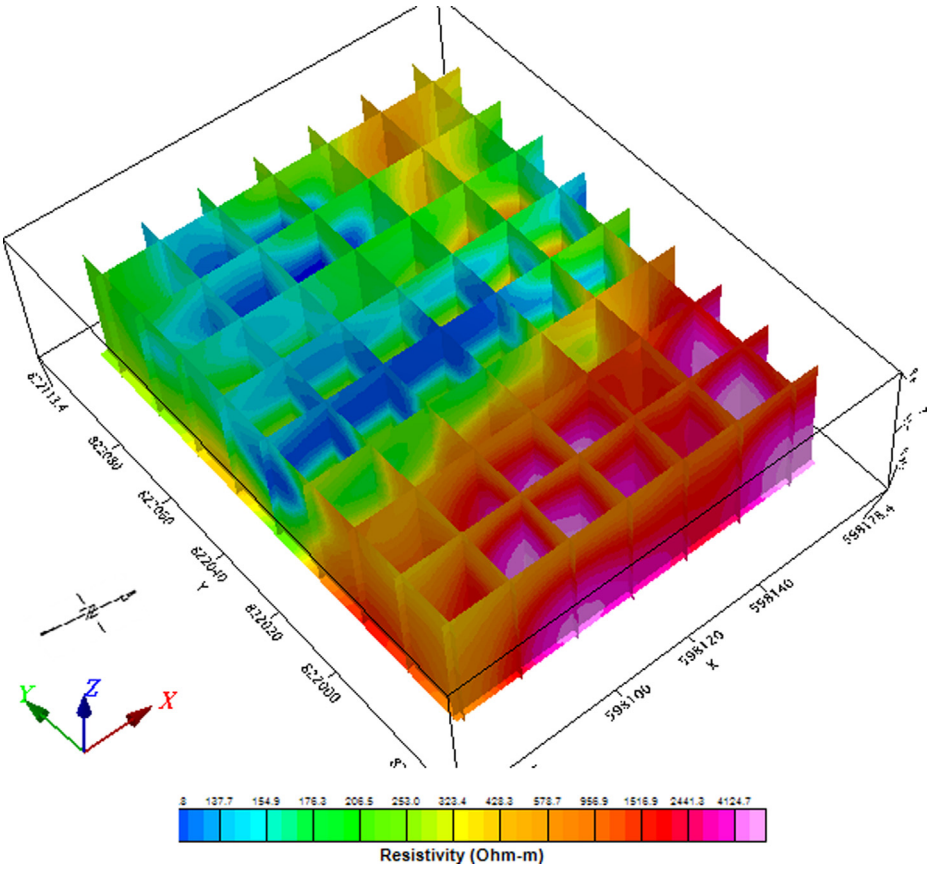

Fig. 6. 2D georesistivity sections mesh across the study area.

(15–300 Ω m). The resistivity mesh also identified some isolated regions of low resistivity zones (< 110 Ω m) in the western part of the studied field.

Two-dimensional (2D) depth resistivity maps present the georesistivity distribution across the entire field at a specified depth. Here, all georesistivity data points from all the occupied profiles, corresponding to the same inverted depth point were sorted and extracted to generate each 2D resistivity map of the study area. Fig. 7 presents the stacked 2D georesistivity distribution maps generated for different depths, right from near the surface (< 1 m) to about 30 m below the ground surface. The stacked resistivity maps indicate the ground resistivity distribution across the field. The individual 2D resistivity depth maps are presented in Fig. 8(a)–(f)

The 2D georesistivity maps of the proposed engineering construction site indicates the resistivity distribution pattern across the field at different depths and these enabled the evaluation of the resistivity distribution pattern of the entire field at different depths. Fig. 8a presents the field resistivity distribution at very close to the surface (< 1.0 m), while Fig. 8(b)–(g) present resistivity distribution across the field at 5, 10, 20, 25 and 30 m depths, respectively. The 2D resistivity

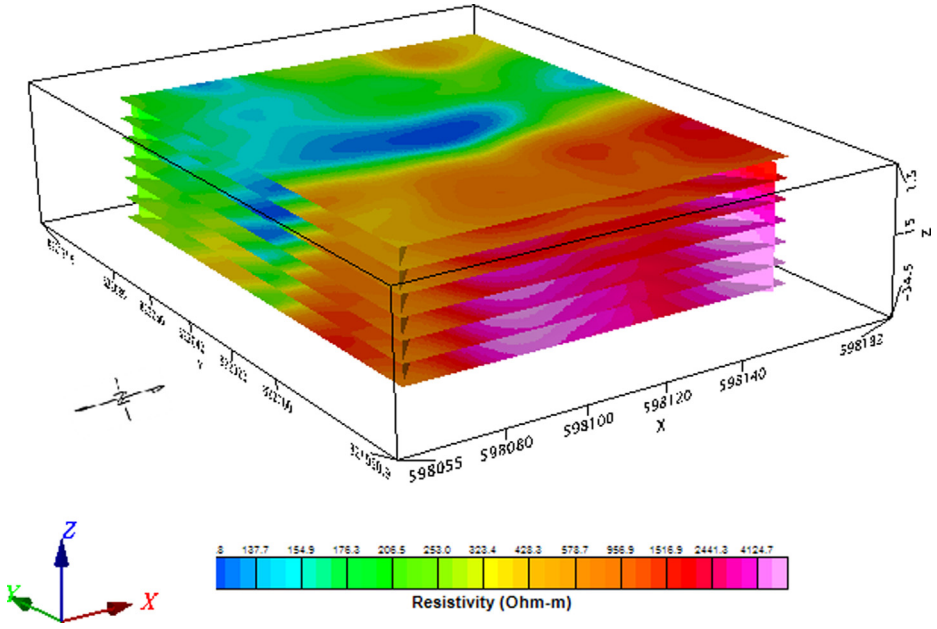

Fig. 7. Stacked 2D georesistivity map of the field at different depths.

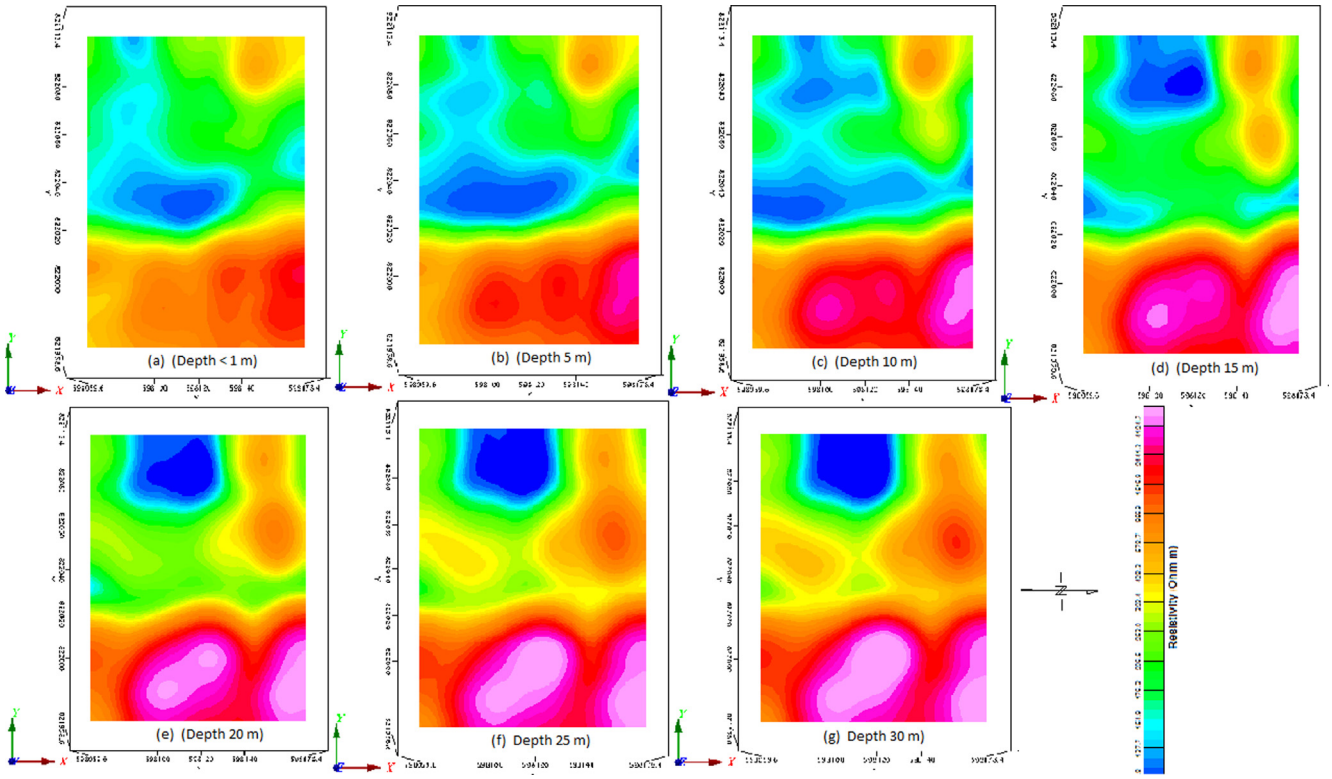

Fig. 8. 2D georesistivity distribution maps of the field at different depths.

distribution maps corroborates the earlier mentioned higher resistivity distribution pattern in the eastern part of the field relative to the west as presented by the georesistivity sections (Figs. 5 and 6). The maps also identified low resistivity zone towards the western part of the site. The various depth resistivity distribution maps indicate increase is ground resistivity value with depth at the eastern part of the field as the resistivity value increases from 450 Ω m at near the ground surface to greater than 4500 Ω m at 30 m depth. The western part of the field on the other hand displayed slightly varied resistivity distribution with some low resistivity zones which dominate the central and the extreme western end of the field. The resistivity distribution in the field ranges from 8 Ω m to 350 Ω m. Low resistivity distribution zone (8–35 Ω m) characterises the south-western part (left hand side) of the field. This zone appears to increase in prominence with depth up till about 10 m as the spread/distribution of the low resistivity zone increases northward as well as westward (Fig. 8).

At deeper depth beyond 10 m, the low resistivity zones become restricted to the extreme west of the field which presents very low resistivity value (< 10 Ω m). The resistivity of the low resistivity zone is generally observed to decrease with depth from 25 Ω m at 15 m to less

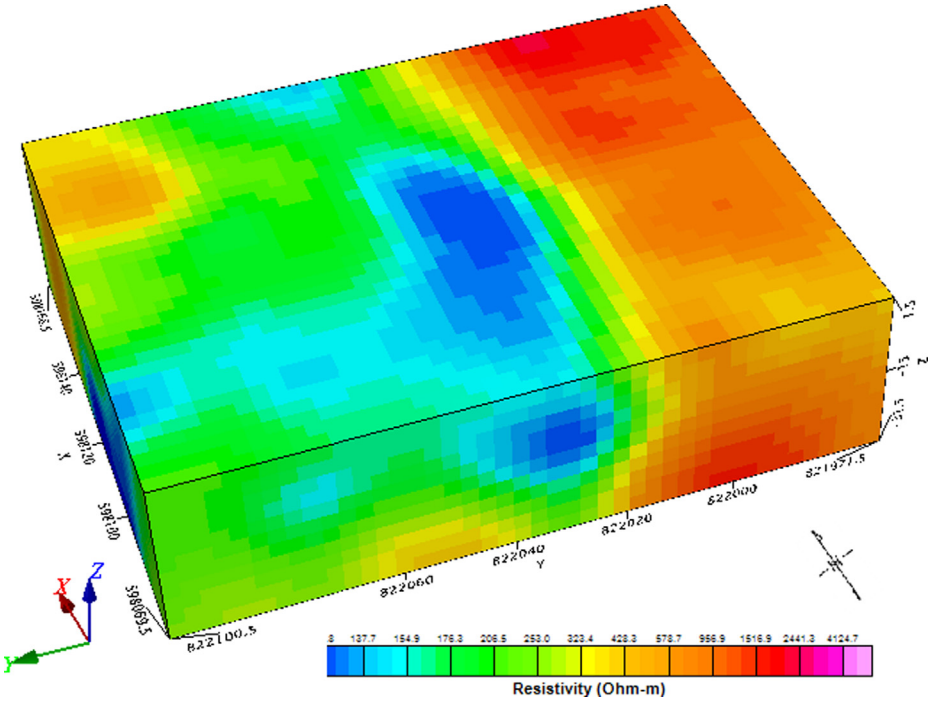

Fig. 9. 3D Georesistivity distribution model of the proposed engineering construction site.

than 8 Ω m at 30 m (Fig. 8).

The summary of ground resistivity distribution of the proposed engineering construction site along three orthogonal directions (x, y & z) is presented in Fig. 9 as 3D subsurface georesistivity distribution model of the field. The 3D model presents the combined georesistivity distribution of all inverted resistivity data from all the occupied ten (10) geoelectric profiles. The figure indicate the variation in ground resistivity distribution along the E–W and N–S directions as well as show variation in subsurface resistivity with depth from the surface to up 30 m below the ground surface. The figure indicate relatively high ground resistivity (450–4500 Ω m) in the eastern part of the field while the western end displayed lower resistivity values (10–50 Ω m). The eastern part of the field displayed consistently relatively high resistivity distribution right from the surface to a depth of about 30 m with resistivity distribution ranging from 450 to 4500 Ω m. The resistivity distribution in the east of the field increases with depth with the deepest part presenting resistivity distribution in excess of 4300 Ω m, which could be attributed to fresh basement resistivity signature. However, the resistivity distribution in the west end of the field varies from medium to low resistivity (10–600 Ω m). The central part of the field presents significantly low resistivity value (10–60 Ω m) which decreases with depth. The low resistivity zone extends in spread north and westward.

5. Discussion of results

The carefully planned 3 dimensional survey through sets of equally spaced parallel survey profile lines along which geophysical data were acquired enabled the generation of grid of data which shows distribution and variation of ground resistivity data along the two horizontal (x & y) and a vertical (z) orthogonal directions. The variation along the vertical is made possible by measurements along the electrical survey levels where based on continuous increase in electrode spacing from one level to another, the sampling depth increases with electrode spacing. The distribution of subsurface resistivity value has been presented as 2D resistivity sections and maps as well as 3D resistivity model across the studied field. The presented subsurface georesistivity models show how the ground resistivity value varies across the field. From the presented sections, maps and models, it is obvious that the subsurface, up to the imaged depth of 30 m, is not uniform in terms of resistivity distribution (Figs. 4–9). This is apparent as the eastern part of the field presented significantly higher resistivity values than the western part of the field. Isolated low resistivity zones which characterises part of the central and western end of the studied field also alluded to this variation. Furthermore, variation in the resistivity values with depth which characterises both the resistive and less resistive zones in the eastern and western parts of the field respectively further confirm spatial variability of ground physical parameter along the three orthogonal directions.

Several factors have been reported to impact variation of electrical resistivity of the subsurface. These include variation in rock type, rock deformation, rock fabrics, different degree of weathering and water saturation among others (Ward & Fraser, 1967; Zonge, 1972). These factors which are known to impact spatial variation on ground electrical resistivity are also capable of impacting variation in other rock's physical properties (Utset & Castellanos, 1999; Carroll & Oliver, 2005). For example variation in ground resistivity distribution which arises due to rock deformation or weathering could also impact variation in the rock density which may in turn affects the bearing strength of the rock unit to efficiently support the load of the building imposed upon it (Chandler, 1972; Tiwari & Marui, 2005).

Geotechnical investigation which has the capacity to directly measure ground's strength to bear the burden of the proposed load is often expensive and labour intensive, thus few points are often selected under assumption that the subsurface is uniform. This assumption is far from reality as subsurface physical properties could vary along both vertical and horizontal directions within short distance (few meters). Adequate subsurface information is essential for site selection and also important to design foundation that would adequately support the intended load of the engineering structure. The best investigation that would aid good foundation design is such that would not only sample the subsurface but also account for spatial variability in the distribution of physical properties of the ground. The result obtained from carefully planned 3D geophysical investigation of proposed engineering construction site could aid point selection in order to capture different zones as presented by the 3D georesistivity model of the subsurface. This way, both

the measured ground resistivity parameter and the vertical as well as lateral spatial variation would be accounted for.

6. Conclusion

The ability of geophysical investigation to measure both subsurface physical parameters such as ground resistivity, as well as determine the spatial variation of the measured parameter along the three orthogonal directions has been demonstrated. The generated sections, maps and 3D models of the subsurface have provided relevant information which is able to guide point selection for geotechnical investigations, especially where the budget is limited and every part of the field could not be covered at very close grid. Geotechnical sampling along carefully selected points and along different delineated varying georesistivity zones, would provide relevant information that would account for heterogeneity of the subsurface and thus guide design of appropriate foundation that will support every part of the building amidst possible variation in rock strength.

References

Amanambu, A.C., 2015. Geogenic contamination: Hydrogeochemical processes and relationship in shallow aquifers of Ibadan, SW Nigeria. Bull. Geogr. Phys. Geogr. Ser. 9, 5–20.

Auken, E., Christiansen, A., 2004. Layered and laterally constrained 2D inversion of resistivity data. Geophysics 69 (3), 752–761.

Badmus, B.S., Akinyemi, O.D., Olowofela, J.A., Folarin, G.M., 2012. 3D electrical resistivity tomography survey for the basement of the Abeokuta terrain of Southwestern Nigeria. J. Geol. Soc. India 80, 845. https://doi.org/10.1007/s12594-012-0213-x.

Burke, K.C., Freeth, S.J., Grant, N.K., 1976. The structure and sequence of geological events in the Basement Complex of Ibadan area, Western Nigeria. Prec. Res. 3 (6), 1976.

Burke, K.C., Dewey, F.J., 1972. Orogeny in Africa in Afr. Geol. Ibadan. Ibadan Univ. Press, pp. 583–608.

Carroll, Z.L., Oliver, M.A., 2005. Exploring the spatial relations between soil physical properties and apparent electrical conductivity. Geoderma 128, 354–374.

Chandler, R.J., 1972. Lias clay: weathering processes and their effect on shear strength. Geotechnique 22 (3), 403–431.

Cho, S.E., 2007. Effect of spatial variability of soil properties on slope stability. Eng. Geol. 92 (3–4), 97–109.

DeGroot-Hedlin, C., Constable, S.C., 1990. Occam's inversion to generate smooth, two-dimensionalmodels from magnetotelluric data. Geophysics 55, 1613–1624.

Ede, A.N., 2010. Building collapse in Nigeria: the trend of casualties in the last decade (2000–2010). Int. J. Civ. Environ. Eng. 10 (6), 32–42.

El-Kateb, T., Chalaturnyk, R., Robertson, P.K., 2003. An overview of soil heterogeneity: quantification and implications on geotechnical field problems. Can. Geotech. J. 40 (1), 1–15.

Fishman, Y.A., 1979. Effect of geological factors upon the pattern of failure and the stability of rock foundations of concrete dams. Bull. Int. Assoc. Eng. Geol. 20, 18. https://doi.org/10.1007/BF02591235.

Folagbade, S.O., 2001. Case studies of building collapse in Nigeria. In: Proceedings of a Workshop on Building Collapse, Causes, Prevention and Remedies, The Nigerian Institute of Building, Ondo State Chapter, pp. 23–24.

Grant, N.K., 1971. South Atlantic, Benue trough and Gulf of Guinea Cretaceous triple junction. Bull. Geol. Soc. Am. 82, 2295–2298.

Jones, H.A., Hockey, R.D., 1964. The geology of part of southwestern Nigeria. Geol. Survey Nig. Bull. 31, 101–104.

Keller, G.V., Frischknecht, F.C., 1966. Electrical Methods in Geophysical Prospecting. Pergamon Press, Oxford.

Loke, M.H., 2001. Topographic modelling in resistivity imaging inversion. In: 62nd EAGE, Conference & Technical Exhibition Extended Abstracts, D-2.

Loke, M.H., 2000. Electrical imaging surveys for environmental and engineering studies, a practical guide to 2D and 3D surveys, geoelectrical.com.

Loke, M.H., Barker, R.D., 1996. Rapid least-squares inversion of apparent resistivity pseudosections by a quasi-Newton method. Geophys. Prospect. 44, 131–152.

Loke, M.H., Chambers, J.E., Rucker, D.F., Kuras, O., Wilkinson, P.B., 2013. Recent developments in the direct-current geoelectrical imaging method. J. Appl. Geophys. 95, 135–156.

Matawal, D.S., 2012. The challenges of building collapse in Nigeria. In: Proceedings of National Technical Workshop on Building Collapse in Nigeria: curbing the incidences of building collapse in Nigeria, pp. 3–54.

Nobahar, A., Popescu, R., 2001. Some effects of soil heterogeneity on bearing capacity of shallow foundations. In: Proc. of ASCE Special Conference.

Olayanju, G.M., Mogaji, K.A., Lim, H.S., Ojo, T.S., 2017. Foundation integrity assessment using integrated geophysical and geotechnical techniques: case study in crystalline basement complex, southwestern Nigeria. Jour. Geophy. Eng. 14 (3).

Olea, R.A., 1974. Optimal contour mapping using universal kriging. J. Geophys. Res. 79, 696–702.

Olorunfemi, M.O., Mesida, E.A., 1987. Engineering geophysics and its application in engineering site investigation – case study from Ile-Ife area. Nigerian Eng. 22, 57–66.

Osinowo, O.O., Akanji, A.O., Akinmosin, A., 2011. Integrated geophysical and geotechnical investigation of the failed portion of a road in Basement Complex terrain, southwestern Nigeria. RMZ – Mater. Geoenviron. 58 (2), 143–162.

Oyawoye, M.O., 1972. The basement complex of Nigeria. In: Dessauvagie, T.F.J., Whiteman, A.J. (Eds.), African Geology. Ibadan Univ. Press, Nigeria, pp. 67–99.

Palacky, G.V., 1987. Resistivity characteristics of geologic targets. Electromagn. Methods Appl. Geophys. 1, 1351.

Rahaman, M.A., 1976. Review of basement geology of south western Nigeria. In: Kogbe, C.A. (Ed.), Geology of Nigeria. Elizabethan Pub. Lagos, Nigeria, pp. 41–58.

Sasaki, Y., 1989. Two-dimensional joint inversion of magnetotelluric and dipole-dipole resistivity data. Geophysics 54, 254–262.

Sharma, P.V., 1997. Environmental and Engineering Geophysics. Cambridge University Press, pp. 173.

Shakleton, R.M., 1976. Pan African structures. Phil. Trans. R. Soc. Lond. A 280, 491–497.

Swain, C.J., 1976. A FOTRAN IV program for interpolating irregularly spaced data using the difference equations for minimum curvature. Comput. Geosci. 1, 231–240.

Telford, W.M., Geldart, L.P., Sheriff, R.E., 1990. Applied Geophysics, second ed. Cambridge University Press.

Terzaghi, K., Peck, R.B., Mesri, G., 1996. Soil Mechanics in Engineering Practice, 3rd ed.,. John Wiley Sons Inc.

Tiwari, B., Marui, H., 2005. A new method for the correlation of residual shear strength of the soil with mineralogical composition. J. Geotech. Geoenviron. Eng. 31 (9), 1139–1150.

Utset, A., Castellanos, A., 1999. Drainage effects on spatial variability of soil electrical conductivity in a vertisol. Agric. Water Manag. 38 (3), 213–222.

Ward, S.H., Fraser, D.C., 1967. Conduction of electricity in rocks: in Mining Geophysics, Vol. II, Theory: Society of Exploration Geophysicists, pp. 197–223.

Webring, M.W., 1981, MINC: a gridding program based on minimum curvature: U.S. Geological Survey Open File Report 81-1224, 41p.

White, R.M.S., Collins, S., Loke, M.H., 2003. Resistivity and IP arrays, optimised for data collection and inversion. Explor. Geophys. 34, 229–232.

Zonge, K.L., 1972. Electrical Parameters of Rocks as Applied to Geophysics. The University of Arizona Ph.D. dissertation.